Back to the deformation and Stress Change Modeling home page

Online Southern California earthquake catalog

Clickable map of the events

R. S. Stein and T. C. Hanks,
M > 6 Earthquakes in Southern California during the Twentieth Century: No Evidence for a Seismicity or Moment Deficit, *Bull. Seismol. Soc. Amer., 88, pp. 635-652, 1998.*
[Online article] [Clickable map and Catalog of earthquakes in Southern California] [Reviews of this paper Nature, Science and Science News Online]

M≥6 Earthquakes in Southern California During the 20th Century:

No Evidence for a Seismicity or Moment Deficit

Ross S. Stein and Thomas C. Hanks
U.S. Geological Survey
Menlo Park, California
(rstein@usgs.gov, thanks@usgs.gov)

Abstract. A broadly based report on seismic hazards in southern California (WGCEP, 1995) concluded that the predicted seismicity exceeds that observed since 1850; a subsequent independent analysis argued that infrequent huge (**M**>8) earthquakes are needed to explain the low rate of large earthquakes (Jackson, 1996). Frequency-magnitude relationships and earthquake reporting suggest that the 1903-1997 catalog we present here, with a *b* value of 1.0 and a rate of **M≥**6 shocks of 0.42-0.49 yr-1, is nearly complete. In contrast, the 1850-1994 catalog used by WGCEP is incomplete before the turn of the century, and thus its reported seismicity rate of 0.32 **M≥**6 shocks yr-1 is too low. Principally because the WGCEP (1995) model results in *b* values of up to 4.0 for regions of lesser and blind faults, the rate of **M≥**6 shocks off the San Andreas system predicted by the WGCEP (1995) model is three times greater than that observed in this century. Because they obtained *b*=0.4 for **M**<7.3 and *b*=2.2 for **M≤**7.3 on major faults, their expected rate of **M≥**7 San Andreas shocks is twice as high as observed. Thus part of the seismicity and moment discrepancy identified by WGCEP was caused by use of an incomplete catalog, and part was caused by inappropriate *b*-values. We obtain a southern California moment release rate of 8-12 x 1018 Nm yr-1,

which cannot be distinguished from the moment release estimated by fault slip, or the moment accumulation inferred from plate motions or geodetically measured shear strain. We thus find no evidence for a moment deficit, significant aseismic moment release, or for rare **M≥8** earthquakes off the San Andreas fault system. Finally, the number of **M≥**6 earthquakes per decade does not depart significantly from a Poisson process during this century, and thus we find no evidence that the rate of seismicity is increasing, now or at any other time since 1900.

Introduction

Southern California seismicity is distributed across a diffuse plate boundary on a mosaic of strike-slip and thrust faults. In a significant advance of the science of seismic hazard analysis, WGCEP (1995) incorporated seismic, geologic, and geodetic data to determine the expected rate of occurrence and distribution of **M≥**6 earthquakes in southern California, reaching the following provocative conclusions:

> * The predicted rate of **M>**6 earthquakes is twice that observed since 1850, implying that the earthquake rate must rise in the future. This precipitated a conference for the insurance industry focused on whether the rate of earthquakes in California is increasing (SCEC, 1996).
>
> * The deficit of historical earthquakes identified by WGCEP (1995) is principally on faults with low or unknown slip rates, and so this is where the rate should rise most sharply.
>
> * The rate of **M**=7.0 earthquakes predicted by the WGCEP model is also twice that observed since 1850, while the rate predicted for **M**=7.9 events is less than half of that inferred from paleoseismology. This low rate of the largest earthquakes makes a moment deficit implicit in the WGCEP model; the moment deficit was explicitly identified by Jackson (1996), who argued for the occurrence of "huge" but rare events.

These findings have had profound effects on earthquake hazard and risk assessment in southern California. Because the predicted long-term rate of **M≥**6 and **M≥**7 earthquakes is twice that experienced during the past 150 yr, the hazard prescribed by WGCEP (1995) is higher than in past estimates (WGCEP, 1988). If huge earthquakes strike the region, then the maximum losses suffered in a single event would be much higher than previously assumed.

M≥ 6 shocks are ten times more abundant than **M≥**7 shocks, so the catalog seismicity rate depends almost exclusively on the smallest earthquakes included, and thus on whether all **M**=6 shocks that occurred are in the catalog (whether the 'catalog is complete' at **M**=6). But because **M≥**7 earthquakes release about 85% of the seismic moment, the seismic moment rate depends almost exclusively on accurate moment estimates of the largest shocks in the catalog. Thus the earthquake rate and seismic moment rate are nearly independent, and one can weigh the WGCEP (1995) findings separately.

Attempts to validate arguments that the rate of earthquakes is increasing through analysis of the more abundant **M**<6 earthquakes have been equivocal. Hutton and Jones (1993) studied $M_L \geq 5$ events since 1932, finding no significant region-wide rate changes. Sykes (1996), in contrast, argued that the rate of both **M≥**5 and **M≥**6 shocks was higher in 1985-1994 than during the previous 9-year period, suggesting that this could be a long-term precursor to a great earthquake. Examining still smaller shocks, Jones and Hauksson (1997) found a high rate of $M_L \geq 3$ events during 1945-52 and 1969-92, and a low rate in 1952-69 and 1992-96. But because nearly all of Jones and Hauksson's significant rate changes are associated with large earthquakes, these results are sensitive to the algorithm used to remove aftershocks (or to 'decluster the catalog').

We thus re-examined the **M≥**6 southern California catalog, focusing on its completeness, the spatial and temporal variability of seismicity, and estimates of the seismic loading imposed by plate motions and released by earthquakes. We sought answers to four questions: Is there an earthquake deficit at any magnitude from 6 on up? Is there a deficit in the release of seismic moment? Is the rate of **M≥**6 earthquakes increasing? And is there evidence for huge but rare earthquakes off the San Andreas fault? We find the answer to all four questions to be no.

1903-1997 M≥6 Earthquake Catalog

The **M≥**6 earthquake catalog presented here (Table 1, Fig. 1, and Appendix) draws upon earlier compilations (Allen et al., 1965; Deng and Sykes, 1997; Ellsworth, 1990; Hanks et al., 1975; Press and Allen, 1995; Richter, 1958; Toppozada, 1988; WGCEP, 1995), although each catalog differs in geographical limits, time periods, and magnitude assessments. Of these, Press and Allen (1995) is most valuable for its inclusion of **M≥**5.5 earthquakes, and Deng and Sykes (1997) for its wealth of focal mechanisms.

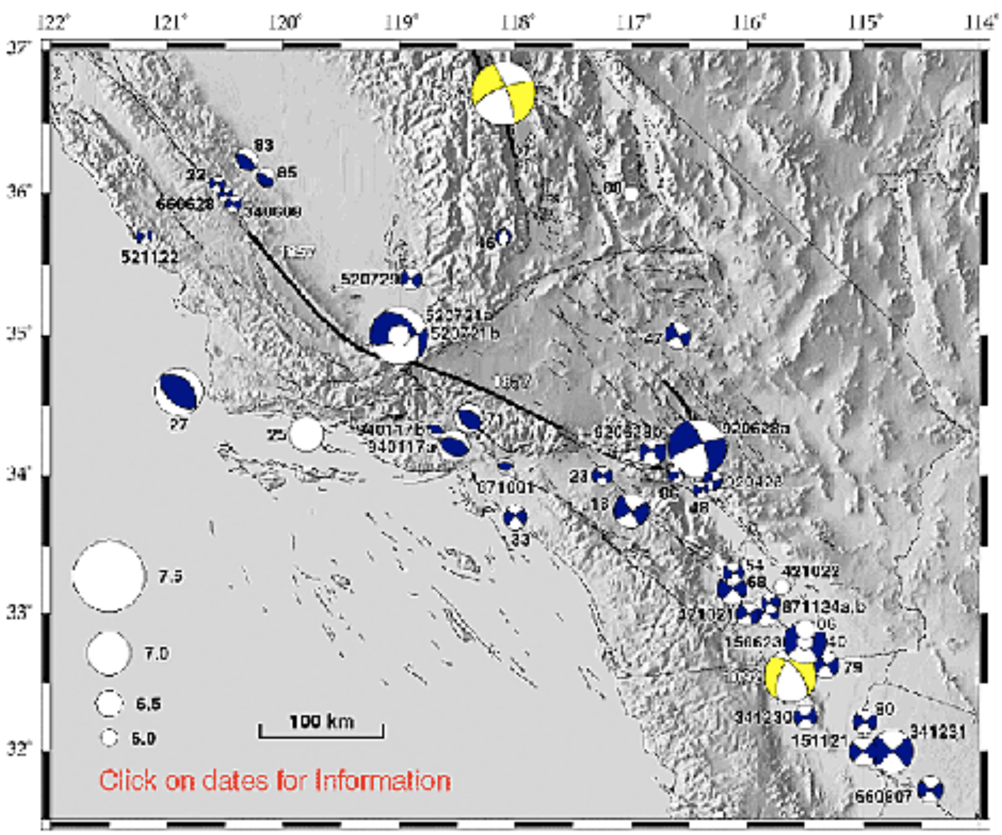

Fig. 1(about 211 kb). **M≥**6 earthquakes in southern California since 1903, with focal mechanisms shown if known. **M≥**7 shocks during 1850-1903 are shown with gray/white focal mechanisms, and surface ruptures for all **M≥**7 shocks are shown as bold black lines. Symbol size is approximately equal to the earthquake source dimension. The bounding latitudes of our **M≥**6 1903-97 catalog (Table 1) are shown as white lines; the bounding longitudes are along the left and right margins of the map. Earthquakes immediately outside the bounding box (1872 Owens Valley and 1966 El Golfo shocks) are also shown.

Our principal goal is for a catalog complete for **M**≥6. Following Richter (1958), we start our catalog in 1903 because instrumental records are available for all of the listed earthquakes. Table 2 lists events excluded from our catalog; Richter (1958) assigned *M*=6-61/4 to the first eight events in Table 2, but more recent analyses indicate they are **M**<6. We examine the region bounded by 32°00'-36°15'N and 114°00'-122°00'W. WGCEP (1995) cited latitude limits of 32°00'-36°00'N, but since they included the Coalinga earthquake at 36°14'N, we moved our northern boundary to include this event as well. For their seismotectonic zone map, WGCEP (1995) used a polygon with extremities bounded by 32°30'-36°10'N and 114°00'-122°00'W, so we have extended their zones south to 32°00'N to make it consistent with their study area (Fig. 2).

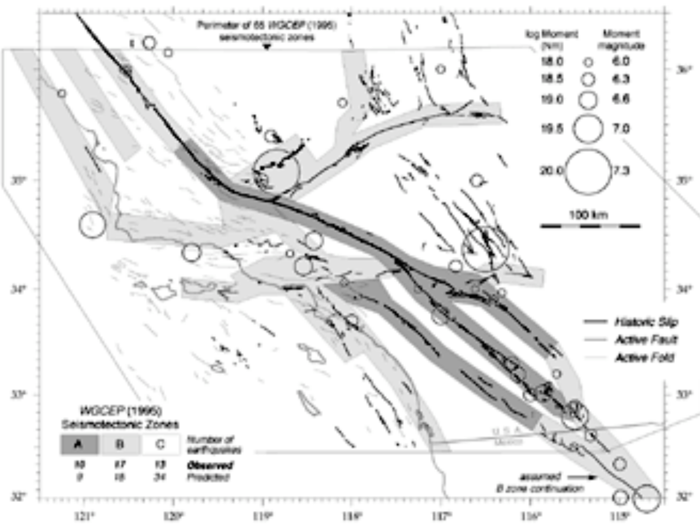

Fig. 2(about 103 kb). **M**≥6 earthquakes in southern California since 1903 plotted on the seismotectonic zones of WGCEP (1995), with symbol size approximately equal to the source dimension. The number of earthquakes falling within the three types of WGCEP source zones is tallied in the inset.

Historical Earthquake Deficit?

Frequency-Magnitude Relationship

Frequency-magnitude curves describe the number of earthquakes expected as a function of magnitude, and enable an assessment of catalog completeness. The curves for our 1903-97 catalog and the WGCEP 1850-1994 catalogs are shown in Fig. 3. The best fit line for each catalog is of the form

$$\log N = a - b\mathbf{M} \quad (1)$$

the standard Gutenberg-Richter representation. For the **M**≥6.0 1903-97 catalog, maximum likelihood estimation (Aki, 1965) yields b=0.97±0.15; least squares yields 1.04±0.04 (Table 3). Maximum likelihood is most sensitive to the completeness of the smallest magnitude included; least squares gives the same weight to all magnitudes, and thus provides a better extrapolation for the rate of the largest earthquakes. For **M**≥6.2, b=1.04±0.20 by maximum likelihood and 1.11±0.04 by least squares, suggesting our catalog is not complete at **M**=6.0 from 1903. If we assume, for example, that the catalog is missing just two

M=6.0 earthquakes (a rate of 0.44 yr^{-1}), the **M≥**6.0 catalog would yield *b*=1.01±0.16 by maximum likelihood. We thus find that *b*=1.0 to be the best estimate for our catalog. Such a *b*-value is the theoretical value if earthquakes have a constant stress drop independent of magnitude (Hanks, 1992). Our catalog *b*-value is indistinguishable from the *b*-value of 0.968±0.023 for the same region for **M≥**4.0 earthquakes by Cao et al (1996), and the *b*-value of 0.98 for nearly the same region during 1932-1971 by Hileman et al (1973). It is also consistent with global crustal earthquakes in the Harvard CMT catalog (5.6≤**M**≤7.4), for which *b*=1.07±0.01 (Pacheco et al., 1992). (Note that all cited *b* values are all for total- rather than declustered-catalogs, and all are computed by maximum likelihood unless otherwise stated).

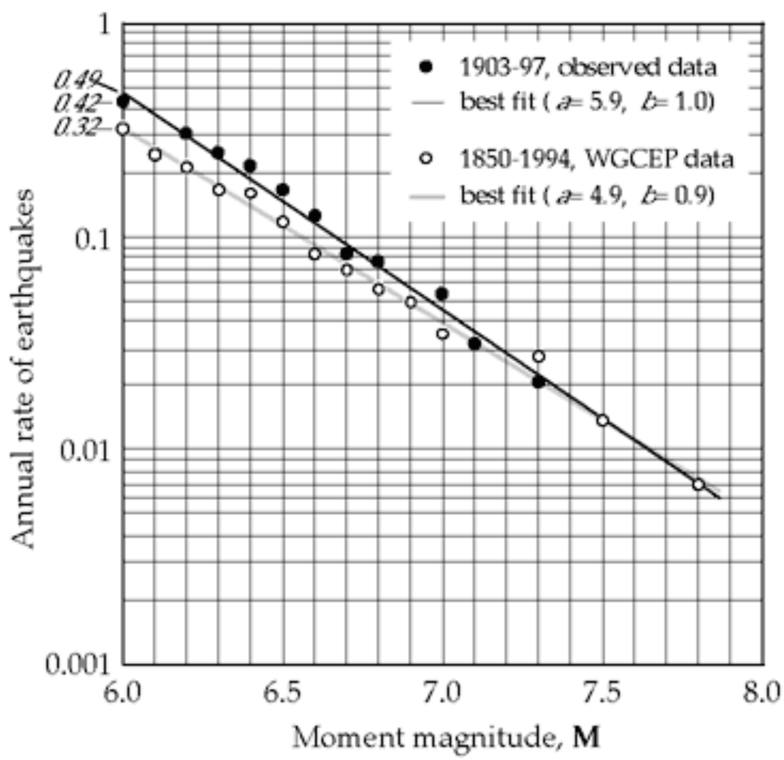

[Fig. 3 (about 18 kb)](). Cumulative number of **M≥**6 earthquakes, expressed as the annual rate, as a function of moment magnitude for the catalog of Table 1 (solid circles), and for the WGCEP (1995) catalog (open circles). The best-fit maximum-likelihood power-law relation yields a *b* value of 1.0 for the 1903-1997 catalog. Note that the 20th century catalog is consistent with the 1850-1994 catalog for **M**>7.3 events. The 1903-97 catalog shows a progressively higher rate of earthquakes for all **M**<7. The WGCEP catalog is incomplete because earthquakes within 32°30'-32°00'N were omitted, and because **M≥**6.5 shocks were under-reported before about 1880-1900.

At Mo = 1 x 1018 Nm, the best fit line suggests the 95-year southern California sample is missing about 3±3 **M≥**6 shocks. Some of these 'missing' earthquakes may be among the 8 events in Table 2 that we judged to be **M**<6.0; two were assigned **M≥**6 by WGCEP. Because any missed earthquakes probably occurred during the first part of the 20th century in the least populated southeastern part of the region, and because these events can contribute at most 10 x 10^{18} Nm or 2% of the 95-year sum, neither the earthquake nor moment rate would change much for their inclusion, with the possible exception of the decade, 1903-1912.

The 1903-97 catalog gives higher rates of seismicity than the WGCEP 1850-1994 catalog for all magnitudes less than 7, with the difference most pronounced for **M≤**6.3. The principal reason for the higher rates of seismicity in our catalog, as we argue below, is insufficient reporting before the turn of the century. A second reason is that WGCEP (1995) omitted all earthquakes south of 32°30'N, despite stating that the catalog extended to 32°00'N. Thus four 6.2≤**M**≤7.0 shocks occurring during 1915-1980 are missing, including two events at 32°00' and two at 32°15' (Fig. 1 and Table 1). Recent analyses of these events by Doser (1994) demonstrates that they lie within the WGCEP study area defined by WGCEP. A third reason is that we re-evaluated and document the seismic moment, location, and focal mechanism of all shocks in our catalog (Appendix), leading to differences in moment assignments. In contrast, WGCEP (1995) cites only Ellsworth (1990) for all pre-1992 shocks.

The rate of **M≥**6.0 shocks from the WGCEP catalog is 0.32 yr-1; the observed rate for the 1903-97 catalog is 0.42 yr-1, and the rate extrapolated from the 1903-97 catalog using the best-fit *b*=1.0 is 0.49 yr-1 (Fig. 4a). If instead we count earthquakes from 1915, the date when Richter (1958) considered the catalog to be complete, the rate becomes 0.46 yr-1, suggesting that our catalog yields a **M≥**6 earthquake rate 44% higher than suggested by WGCEP (1995). Stirling and Wesnousky (1997a) showed that the statistics of a Poisson process are alone sufficient to nullify the WGCEP (1995) claim of a seismicity deficit. This is an important result, but we believe that the deterministic solution to this problem-catalog incompleteness-is even more important, because the observations used by both WGCEP (1995) and Stirling and Wesnousky (1997) were biased by catalog incompleteness before the turn of the century.

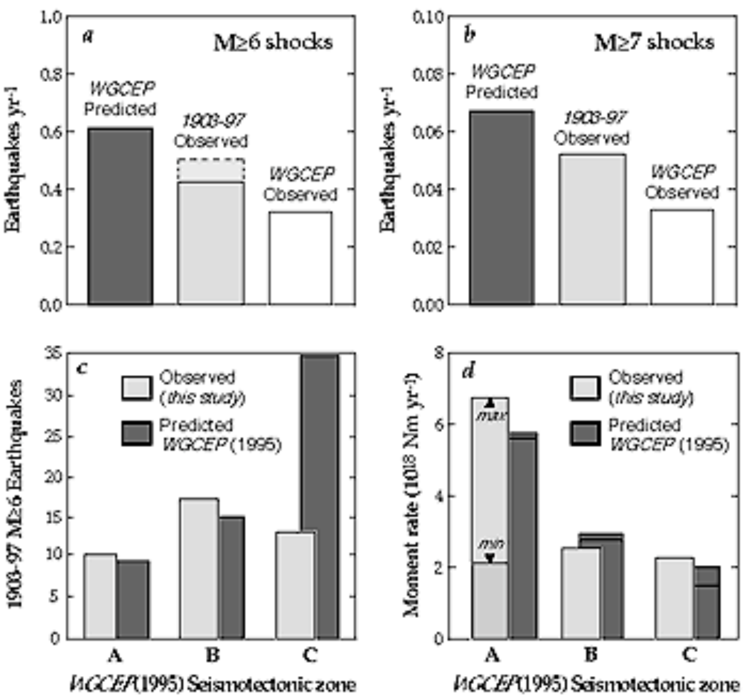

Fig. 4 (about 19 kb). Comparisons of the WGCEP (1995) preferred model with the observed 1903-97 catalog. (*a*) Net rate of **M≥**6 earthquakes. The observed rate is solid; the inferred rate using *b*=1.0 is dashed. (*b*) Net rate of M≥7 earthquakes. (*c*) The observed and predicted number of **M≥**6 earthquakes during 1903-97 by seismotectonic zone. Agreement is good except for the number of shocks on lesser or blind faults, and faults with unknown slip rates (zone C). (*d*) The seismic moment rate. The two lines on the predicted rates portray the 'preferred' and 'alternative' models of WGCEP (1995). The observed rate on major segments of the San Andreas, San Jacinto, and Elsinore faults (zone A) has been augmented for the contribution of an earthquake with a moment equal to the 1857 shock with inter-event time between 125 yr (labeled '*max*') and 500 yr (labeled '*min*').

The rate of **M≥**7.0 shocks from the WGCEP catalog is 0.033 yr-1; the observed rate for the 1903-97 catalog is 0.052 yr-1, 58% higher (Fig. 4*b*). The difference in the rates of **M≥**7 shocks arises because WGCEP omitted the 1934 **M**=7.0 Colorado River delta shock, and identified the 1940 Imperial Valley earthquake as **M**=6.9 rather than **M**=7.0 (Table 1 and Appendix). The WGCEP catalog for 1850-1994 includes five **M≥**7.0 events, a rate of 0.033 yr-1 (Fig. 4*b*). In contrast, we count five **M≥**7.0 events since 1903 (Table 1), and seven since 1850 (Table 2), a rate for both time periods of 0.053 yr-1. (Because the **M**=7.4 1872 Owens Valley earthquake lies north of the WGCEP boundary, it is not included in these rates.) Note that for **M≥**7.3, the annual rate of earthquakes extrapolated from our catalog and that measured by WGCEP converge.

Catalog Completeness

Inadequate to nonexistent reporting of moderate earthquakes in southern California before the turn of the 20th century has been widely studied, and we argue here that this is the principal reason why the WGCEP catalog shows a lower rate of **M≥**6 shock than does ours. Richter (1958) commented that "for the years before 1915 [his *M*≥6 catalog] is almost certainly incomplete." Toppozada et al (1981) found that in several inland southern California counties (San Bernardino, Riverside, and Imperial), **M**=7 shocks could have been inadequately reported for proper identification until about 1870, and **M**=6.5 events could have been improperly identified until the late 1880's. Agnew (1991) concluded that **M≥**6.5 events would have gone unidentified along the southernmost San Andreas and central San Jacinto faults as late as 1870-1880. The reason for these conclusions is simple: while northern California experienced dramatic population growth after the discovery of gold in 1849, immigration to southern California occurred much later (Fig. 5a), with a corresponding delay in the adequate reporting of small earthquakes (Fig. 5b). Before 1875, there were almost ten times more people living in northern than southern California; the population of northern California in 1880 was not attained in southern California until 1910.

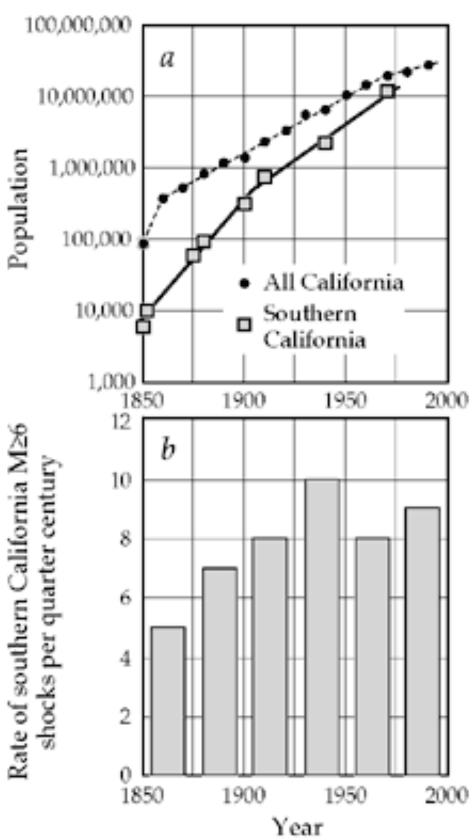

Fig. 5 (about 23 kb). (*a*) Exponential population growth of California since 1850, with southern California distinguished. The population of the northern part of the State in 1880 (~800,000) was equal to the southern California population in 1910. (*b*) The rate of **M≥**6 shocks in the WGCEP (1995) catalog rose between 1850 and early in the 20th century, in concert with the population growth.

Population in southern California was very sparse along the San Andreas system and eastern California shear zone until about 1900 (Fig. 6). In the pre-instrumental era, newspaper reports are the principal source of isoseismal maps used to estimate the size and locations of earthquakes in California (Toppozada et al., 1981). Although earthquakes were mentioned in diaries and letters from sites which lacked newspaper coverage, newspapers are the principal source of data for the pre-instrumental record, and thus limitations in newspaper coverage is reflected in the catalogs. Newspaper coverage closely mirrored the population expansion, with inland population following railroad construction (Fig. 7).

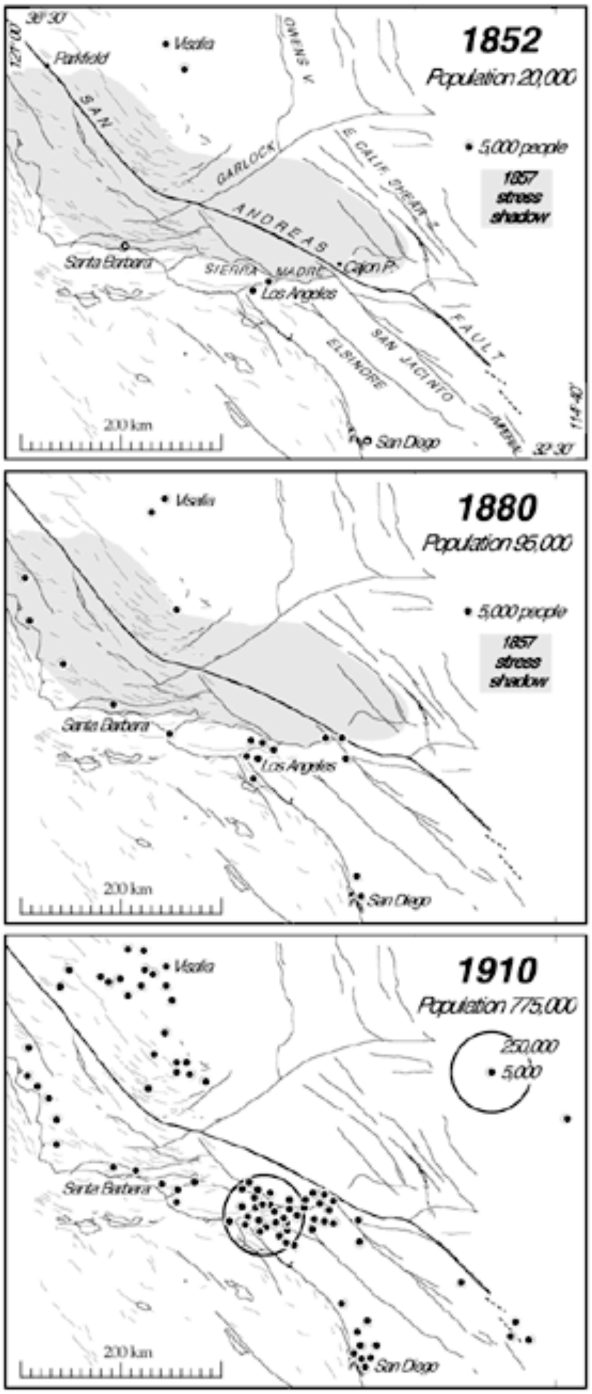

Fig. 6 (about 93 kb). Population distribution in southern California during 1852-1910, from Donley et al (1979). Population and newspaper (Fig. 7) trends are similar, although the federal census data are less frequent. The Coulomb stress decrease (<0.1 MPa), or stress shadow, associated with the **M**=7.9 1857 earthquake (Harris and Simpson, 1996) is shaded. Note that population is sparse within the shadow during 1852-1880.

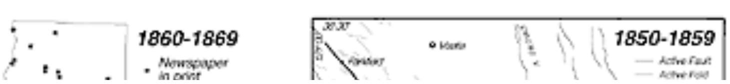

Fig. 7 (about 103 kb). Newspapers in print during

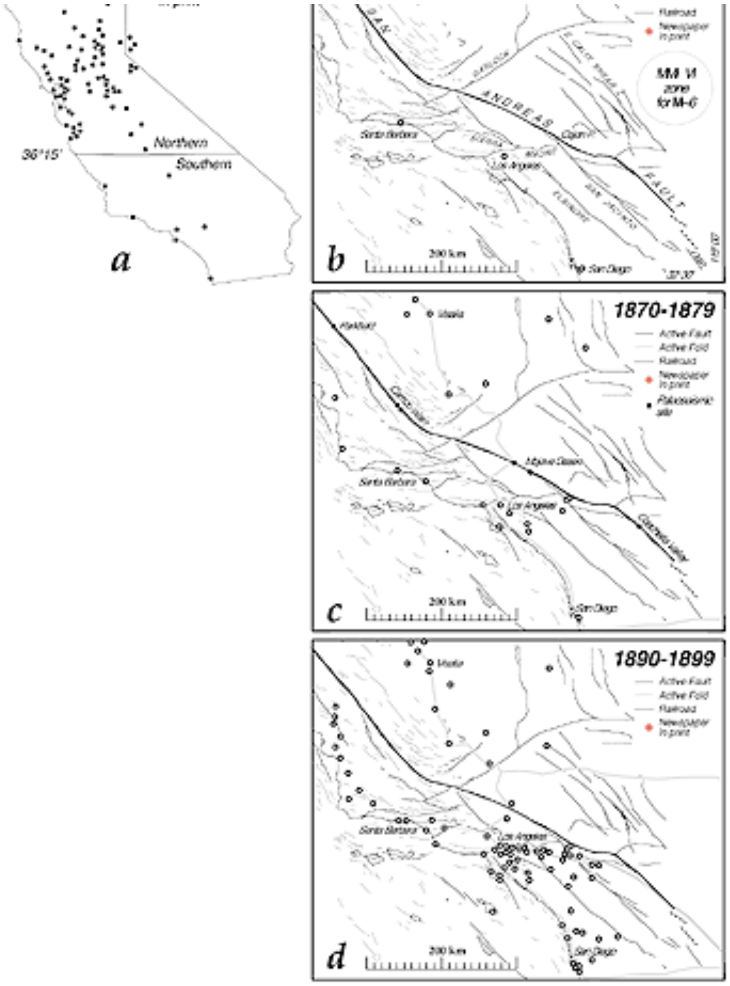

1850-1899, from Toppozada et al (1981), and routes of the Southern Pacific and Sante Fe railways from Donley (1979) and Hart (1978). Newspapers that were in print for at least 5 yr are shown. (*a*) Comparison of coverage throughout the State during the decade after the Gold Rush. (*b*-*d*) Until 1890, there were few newspapers reporting within 75 km of the San Andreas, San Jacinto, Elsinore, Garlock, White Wolf faults, the eastern California shear zone, and the Coastal and western Transverse Ranges folds.

The MMI (Modified Mercalli Intensity) VI isoseismal, which extends 50-60 km from a **M**=6 shock (Hanks et al., 1975; Toppozada, 1975), is generally needed to estimate a size and location (Fig. 7). Before 1880, no southern California newspapers were printed within 75 km of the San Andreas fault except at Cajon Pass. As late as 1890-99, newspapers were printed within 50 km of the San Andreas fault only near the Parkfield, Mojave, and San Bernardino Mountain fault segments (Fig. 7). Consistent with these reporting limitations, no 6.0≤**M**≤6.1 shocks are in the 1850-1994 catalog during the thirty-year period, 1863-1893. Until about 1895, the Elsinore, Garlock, Owens Valley, and Imperial Valley and most of the San Jacinto fault lacked newspapers printed within 100 km, and most of the western Transverse Ranges, the borderland faults, and the eastern California shear zones lacked any coverage at all. Further, many of the pre-1910 newspapers have not survived, and thus are not presently available for isoseismal analysis (Toppozada et al, 1981).

Could the low observed rate of southern California **M**≥6 shocks during 1850-1900 (Fig. 5*b*) instead be a consequence of the 1857 **M**=7.9 earthquake? Harris and Simpson (1996) found that for 50 yr after 1857, at least 10 of the 13 known **M**≥5.5 events were brought closer to failure by the 1857 earthquake, whereas during the succeeding 50 yr, only 13 to 15 of the 23 **M**≥5.5 events were encouraged by the 1857 shock. They concluded that the earthquake-induced stress changes depressed earthquake rates for 50 yr after the 1857 event. However, the zone in which strike-slip faults were brought farther from failure (termed the stress shadow), and where few shocks were seen during 1857-1907, is centered on the San Andreas between Parkfield and Cajon Pass (Fig. 6). Until 1890, there was poor earthquake reporting in the shadow due to lack of population. For example, there are no recorded aftershocks of any magnitude within 40 km the **M**=7.8 1857 event for at least 27 years (Toppozada, 1995), suggesting that **M**≥6 aftershocks went unidentified. The much smaller Kern County and Landers shocks (both **M**=7.3) had two **M**=6.3 aftershocks, and one **M**=6.5 aftershock, respectively. In addition, regions in which the 1857 event increased and decreased the stress should be roughly equal in extent, and thus the overall rate of shocks should have been little changed.

Given the reporting limitations within the stress shadow, only if it could be shown that the rate of shocks during 1807-1857 was higher than during 1857-1907 could the stress shadow be a tenable hypothesis to explain the low **M**≥6 rate before 1900. The limited evidence does not support such an hypothesis: During the 50 yr before the Ft. Tejon earthquake there were four recorded **M**≥6 and two **M**≥6.5 shocks (Toppozada, 1995). During the succeeding 50 yr there were eleven **M**≥6 shocks and three **M**≥6.5 shocks (WGCEP, 1995). Thus even at a completeness level of **M**=6.5, there is no evidence to suggest that the rate of shocks in southern California was depressed by the 1857 event. We consider it highly unlikely that the 1857 earthquake can account for the difference in **M**≥6 earthquake rate between southern and northern California during 1850-1900, or between 1850-1900 and 1900-1950 within southern California.

We thus conclude that the 1850-1995 catalog used by WGCEP (1995) is incomplete for **M**≤6.5 before about 1880-1900 (Fig. 5*b*), rendering its observed **M**≥6 earthquake rate 31-44% too low. This conclusion is far more likely than the possibility that the 1857 stress shadow depressed the rate of earthquakes until the turn of the Century. Our finding is bolstered by the observation that ten times more earthquakes are reported for northern than southern California during 1850-1890, whereas after 1895, the rates of reported shocks rates are about equal (Toppozada et al., 1981). We attribute this difference primarily to the ten-fold population difference between north and south during the same era (Fig. 5).

Earthquake Time Series

While southern California was more active during some decades than others, no interval is statistically anomalous, with the possible exception of 1983-92 (Fig. 8). We bin from the third year of each decade, starting in 1903. The average rate of **M**≥6 shocks is 4.2 per decade. For a Poisson process, the 2s confidence limit on the observed rate is $\pm 2(4.2)^{0.5}$ or 4.2±4.1. Thus 0-8 earthquakes per decade are consistent with a Poissonian process, and only one decade out of ten (9 events fall in 1983-92) exceeds this rate. If we had binned from 1900, the range would be 2-7 per decade and 5 since 1990, and thus no decade would be anomalous. Using the c^2 test (Evans, 1955), there is a 10% probability that still larger excursions from the mean rate would occur if this were associated with a Poisson distribution. Thus there is no evidence from the **M**≥6 catalog that the rate of earthquakes has undergone a significant increase at any time since 1903.

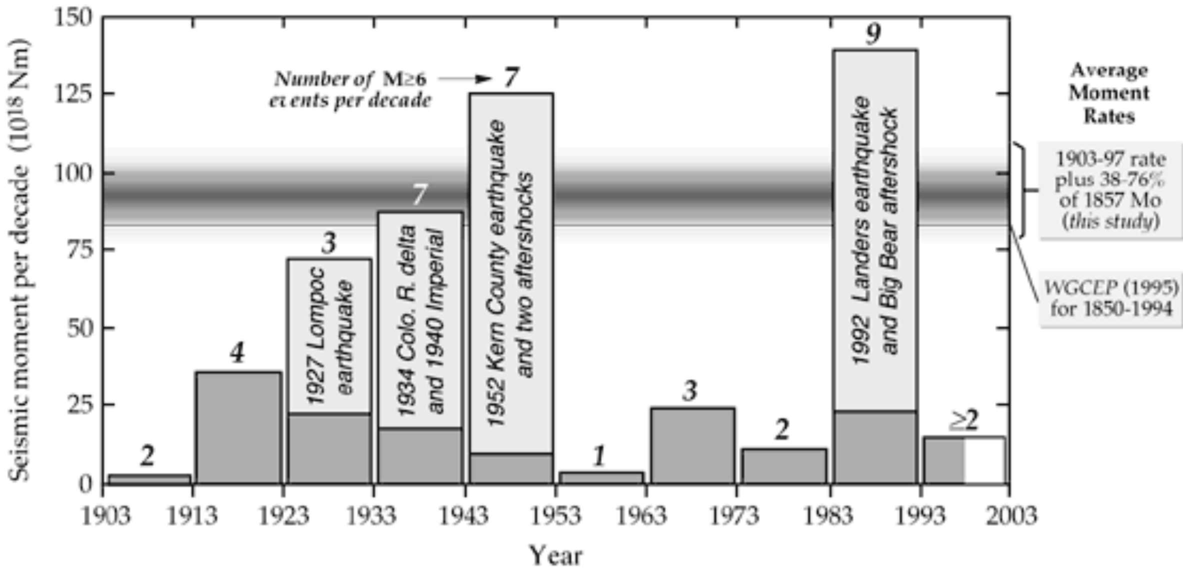

Fig.8 (about 42 kb GIF). Seismic moment and the number of **M**≥6 earthquakes per decade since 1903, with the contribution of **M**≥7 earthquakes and their largest aftershocks distinguished. Large fluctuations of the number of earthquakes from one decade to the next are consistent with a Poisson process.

Historical Seismic Moment Deficit?

Seismic Moment Sums

Summing the effects of two or more earthquakes should proceed by addition of the seismic moment tensors. Because focal mechanisms for some events are unknown or poorly known (Fig. 1), we use scalar seismic moment sums as a gross measure of seismic strain release in southern California. Fig. 8 shows these sums for the nine 10-yr periods since 1903. The accuracy of the seismic moment estimates rests on the ten post-1903 earthquakes with Mo > 1019 Nm in Table 1, for these account for 86% of the moment. Apart from the 1927 Lompoc and the 1925 Santa Barbara shocks, we consider the estimates for the $M_o > 10^{19}$ Nm earthquakes given in Table 1 to be accurate to ±50%, and somewhat better than this for the five most recent events. The uniform slope of the observations in Fig. 3 suggests that we are not likely to have missed even one earthquake of $M_o > 10^{19}$ Nm by grossly underestimating M_o for an event. Apart from the dominance of **M**≥7 shocks in the decade moment sums, it is intriguing that the earthquake moment rate rose steadily for 5 decades from 1903. As we have shown, however, this is based on very few earthquakes and is not statistically significant.

The size and frequency of occurrence of the 1857 Ft. Tejon-type earthquakes (Fig. 1) play a key role in estimating the rate of moment release in southern California. By including the full moment of the 1857 event in the 1850-1994 catalog, WGCEP (1995) implicitly assumed that its inter-event time is equal to the catalog duration, 148 yr. To compare the 1903-97 and 1850-1995 catalog rates to the moment-accumulation rate expected from plate motions, we augment the 1903-97 moment rate to include the effect of larger, less frequent events such as the Ft. Tejon earthquake. To do this we must estimate the seismic moment of the 1857 event (8 x 10^{20} Nm; see Appendix) and its inter-event time.

Paleoseismic studies suggest that large earthquakes have occurred on the southern San Andreas fault with an average inter-event time of 125-250 yr (Grant and Sieh, 1994; Sieh, 1996). The available data suggest inter-event times of 160 yr at two sites in the Carrizo Plain, 125 yr at two sites along the edge of the Mojave desert, and about 250 yr in one site the Coachella Valley (sites shown in Fig. 7c). What, if any, correlation exists between events at these sites is unclear, but the paleoseismic record suggests that the 1857 earthquake is not characteristic: There is evidence for shorter rupture lengths and lower values of slip for several prehistoric events in both the Carrizo Plain and in the Mojave Desert, and for the possibility of events with ruptures longer than occurred in 1857 in about AD 1480 and AD 1000 (Sieh, 1996). The data thus suggest that an earthquake comparable in size to the Ft. Tejon event occurs every 125-250 yr somewhere along the southern San Andreas fault.

We estimate the seismic moment release rate in several ways. First, we sum the seismic moments of the eight **M**≥7 shocks in Tables 1 and 2, divide this by the 148-yr period 1850-1997, and add to this the seismic moment release rate of the 6.0≤**M**≤6.9 shocks observed this century. This assumes a 148-yr repeat time (*RT*) for the 1857 Ft. Tejon shock. Alternative calculations assume a 125-250-yr repeat time for such **M**=7.9 events, calculated with and without the 1872 Owens Valley shock. This yields 7.9-1.1 x 10^{18} Nm yr-1, a broad range but indistinguishable from the WGCEP (1995) moment release rate of 8.3 x 10^{18} Nm yr-1 for 1850-1995 (Fig. 9). This agreement is not surprising, because the moment rate depends principally on the few largest earthquakes, while the earthquake rate depends on the smallest shocks and thus differs between the two catalogs by 44%. If we include the 1872 **M**=7.4 Owens Valley shock, the release rate rises to 9.2-1.24 x 10^{18} Nm yr-1. Although the 1872 shock struck just outside of the WGCEP border (Fig. 1), the earthquake lies athwart the North America-Pacific plate boundary in southern California, and thus is appropriate to include in the moment balance.

Moment Accumulation Rate

The rate of moment accumulation can be inferred from remote plate motions or from the geodetically measured shear strain rate. But estimating the moment rate is complicated by the unknown depth, *H*, over which the strain accumulates. The geodetically inferred locking depth on the southern San Andreas is 25 km, which could be interpreted to be *H*. Savage and Lisowski (1997) explain the apparent 25-km locking depth to be a consequence of viscoelastic coupling with an elastic crust extending to 15 km depth. *H* might thus be set to equal the depth extent of earthquakes (12-15 km), minus the upper ~2 km of the crust in which little elastic energy is believed to be stored, or 10-13 km. But *H* could be 7-10 km if inelastic strain release occurs during the time period between large earthquakes at the base of the rupture, as suggested by studies of the effective elastic thickness of the crust over hundreds of earthquake cycles (King et al., 1988; Stein et al., 1988). Here we assume that *H*=10-12 km; WGCEP (1995) used 11 km but considered this a lower bound.

The simplest estimate of the moment accumulation from plate motions, $\dot{M}_o^p$ is made by resolving the plate motion across southern California.

$$\dot{M}_o^p = m \, \dot{u} LH$$

where $\dot{u}$ is the plate motion rate, L is the length of the fault or trend within the study area parallel to the plate motion vector, 600 km. For $\dot{u}$ at 36°N latitude, Argus and Gordon (1991) obtained 39 mm yr-1 oriented N37°W by removing the Basin and Range opening, DeMets (1995) found 49 mm yr-1 oriented N38°W (NUVEL-1A), and at latitude 33°30', Bennett et al (1996) found 49±3 mm yr-1. We thus use 49 mm yr-1 oriented N38°W. For m = 3.0 x 10^{10} Nm-2 and H = 11 km, M_o^p= 1 x 10^{19} Nm yr-1, slightly higher than the value used by WGCEP (1995). This gives a lower bound because some of the seismic moment is associated with creation of compressional structures by slip on thrust faults (Fig. 9).

Ward (1997) integrated the horizontal velocities of 287 geodetic stations surveyed during 1970-1995 to obtain a southern California strain rate, $\dot{e}$, of 11.8±2.6 x 10^{-8} yr-1. From Kostrov (1974), M_o^s, the moment measured from elastic strains can be written

$$M_o^s = 2mAH\,\dot{e}$$

M_o^s where m is the shear modulus, *A* is the area, and *H* is the thickness over which strain is accumulated and released. For m = 3.0 x 10^{10} Nm-2, and *H* = 11 km, Ward obtained M_o^s= 1.23±0.17 x 10^{19} Nm yr-1 (Fig. 9), 30% higher than the M_o^s value used by WGCEP (1995). Jackson et al (1997) have shown that the distribution of strain is highly concentrated where some of the large earthquakes most recently occurred, suggesting that transient postseismic strain may obscure the long-term strain accumulation.

Moment Release Rate From Fault Slip

A discrete summation of the moment release on all faults with known slip rates and lengths, M_o^f, was carried out by WGCEP (1995) and Ward (1997). This method is subject to the uncertainty on the slip rate of the many minor faults. WGCEP (1995) reported M_o^f= 0.93 x 10^{19} Nm yr-1; using *H*=11 km, Ward (1997) got M_o^f= 1.00 x 10^{19} Nm yr-1 using the improved Petersen et al (1996) fault inventory, which we use here (Fig. 9).

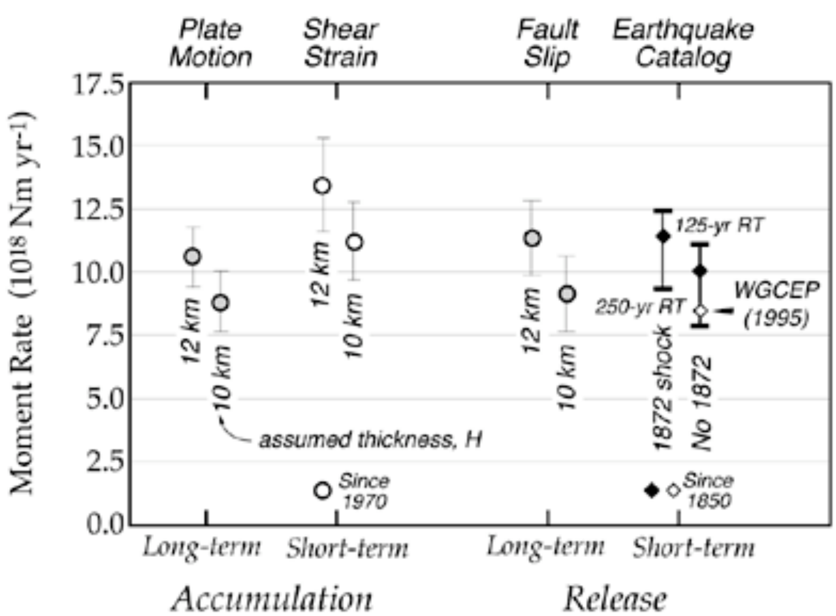

Fig. 9 (about 33 kb GIF). Comparison between the moment accumulation and release rates for long and short time scales. The moment accumulation comes from plate motions (DeMets, 1995) and geodetically measured shear strain (Ward, 1997); the release rate is from late-Quaternary fault slip rates (Petersen et al, 1996) calculated by Ward (1997). Values are shown for an assumed depth extent of moment accumulation, *H*, of 10 and 12 km. The earthquake release rates are for the 1903-97 **M**≥6 catalog augmented by inclusion of the 1857 earthquake, assuming that such San Andreas events have a repeat time (*RT*) of 125-250 yr. The moment release rates since 1850 cited by WGCEP (1995) is shown by the open diamond; our estimates are the solid diamonds. The fault slip and earthquake moment rates are strictly comparable, since both include strike-slip and thrust sources; one can reduce the catalog moment rate by 1.3 x 10^{18} Nm yr^{-1} for comparison to the plate motion.

Balance of Moment Accumulation and Release

When *H* is fixed at 11 km, the two estimates of the moment accumulation rate vary from 9 to 12 x 10^{18} Nm yr-1. For a minimal uncertainty on *H* of 10-12 km, the range expands to 8-13 x 10^{18} Nm yr-1. This can be compared to the moment release rate from fault slip of 8.0-11.5 x 10^{18} Nm yr-1 and a release rate measured by the catalog of 7.9-12.4 x 10^{18} Nm yr-1 (Fig. 9). We thus find no observable difference between the rates of moment accumulation by plate motions and moment release by earthquakes. Irrespective of the particular seismic model advanced by WGCEP (1995) or others, the absence of a significant difference between the rates of moment accumulation and release precludes any statement that there is a deficit in the rate of historical seismic moment.

Spatial Distribution of Earthquakes

Rate Predictions for Seismotectonic Zones

To understand why and where WGCEP (1995) predicted higher earthquake rates than observed during this century, we examine the distribution of the earthquakes in Table 1. WGCEP divided southern California into 65 seismotectonic zones, based on fault activity and the extent of knowledge in each region (Fig. 2). The A zones include major segments of the San Andreas, San Jacinto, and Elsinore faults (by area, 7% of southern California); the B zones include major faults with known slip rates, such as the Garlock and Newport-Inglewood (15%); the C zones include lesser or blind faults, and faults with unknown slip rates (78% by area).

The WGCEP (1995) predicted a rate of moment release in each of the 65 seismotectonic zones. WGCEP states that the rate of distributed earthquakes was assigned under the assumption that b=1.0 in equation (1) in all zones, but this is only true for the discrete magnitude distributions. For the cumulative distributions presented here and in their report, $0.4 \leq b \leq 4.0$ in different magnitude bands (Fig. 10). Equation (1) was modified by WGCEP (1995) so that the rate of earthquakes approaches zero at a limiting magnitude, **M**x, which they supplement with additional events of magnitude **M**x (the 'characteristic' earthquakes) occurring at an assigned frequency, *f*c. In the A zones, *f*c was set to the rate of characteristic earthquakes determined from geologic data, and *a* in (1) was based on the rate of **M**≥6 shocks with characteristic earthquakes removed. The characteristic earthquakes were instead represented by the moment associated with the fault slip in these zones. In the B zones, *a* was based on the rate of all **M**≥6 shocks, and *f*c was set so that the predicted moment rate equaled the average of the geological (slip-rate based) and geodetic (shear-strain based) moment rates. In the C zones, *f*c was set to zero, and **M**x was related to the mapped faults (or the total length of each zone) by the empirical relations of Wells and Coppersmith (1994). In the C zones, **M**x was assigned values ranging from 6.4 to 7.3, and *a* was based on the average of the smoothed catalog seismicity and the geodetic moment rate.

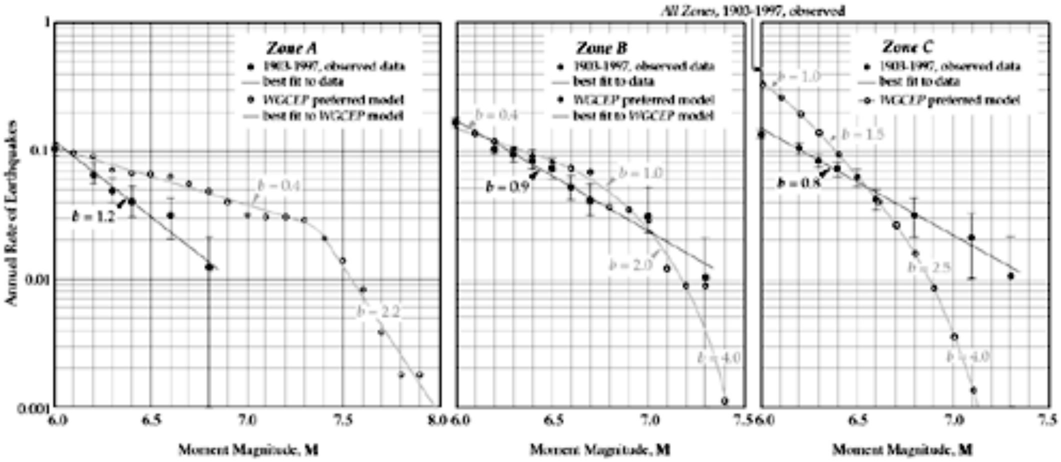

Fig. 10 (about 65 km GIF). Frequency-magnitude relations for earthquakes since 1903 within the WGCEP seismotectonic zones (dots), compared to the WGCEP preferred model (circles). The zone limits are shown in Fig. 2. During 1903-97, 10 shocks fall into A zones, 17 in the B zones, and 13 in the C zones. Note that the *b*-values modeled by WGCEP depart strongly from that observed. The number of earthquakes in the C zones is overestimated by a factor of nearly three. In fact the total number of earthquakes for all zones is close to the prediction for the C zone (bold arrow in *c*). The observations suggest similar distributions for the B and C zones, quite unlike the WGCEP model. The *b* = 0.4 model for the San Andreas shocks (Zone A) is quite inconsistent with the past century of earthquakes in Zone A, or all zones combined.

We compare the 1903-97 catalog distribution of earthquakes with the WGCEP (1995) predictions in Fig. 10. As discussed previously (Fig. 4), our estimate of the rate of **M**≥6 shocks is about 44% higher than the rate reported by WGCEP (1995). But the WGCEP (1995) model predicts a rate of 0.60 **M**≥6 shocks yr-1, 33% higher than our maximum estimated rate of 0.46 yr-1 (Fig. 4*a*). Nearly all earthquake deficit predicted by the WGCEP model is in the C zones (Fig. 4*c*), the site of blind faults or those with low or unknown slip rates. WGCEP (1995) predicts nearly three times the number of earthquakes observed during the past 95 years, even though the past century has produced three large C zone events, the **M**=6.8 Santa Barbara, **M**=7.1 Lompoc and **M**=7.3 Landers shocks.

*Source of WGCEP's **M**≥6 Earthquake Rate Deficit*

Despite the rough agreement between the WGCEP predicted and observed moment rate in the C zones (Fig. 4*d*), there is a large disparity between the predicted and observed earthquake rates (Fig. 4*c*). How can this be? The cumulative frequency-magnitude curve predicted by the WGCEP (1995) model and the curve observed during 1903-97 for all C zones is shown in Fig. 10*c*. In the WGCEP (1995) model, *b*=1 only for 6≤**M**<6.1; *b*=2.5 for 6.5<**M**≤6.9, and *b*=4 for **M**>6.9. In contrast, *b*=0.9 for the observed earthquakes in C zones over the full range of 6≤**M**≤7.3 (Fig. 10c and Table 3). Thus the observed rate of **M**≥6 shocks in the C zones is one-third the rate predicted by the WGCEP model, while the observed rate of **M**≥7 shocks is much higher than predicted by WGCEP. In fact the predicted rate of **M**≥6 shocks in the C zones is close to the observed rate for zones A, B, and C combined (shown by the black arrow in Fig. 10*c*), a highly unlikely scenario. Both observed and predicted curves yield similar seismic moments, because for *b*-values greater than 1.5, smaller earthquakes contribute more moment than larger ones. Thus the WGCEP model for C zones bears no resemblance to the observed earthquake occurrence in this century; the evidence favors an inappropriate model *b*-value rather than an earthquake deficit on the minor and blind faults.

Source of WGCEP's Large-Earthquake Deficit

The frequency-magnitude relations assumed in the WGCEP model differ substantially from the observed catalog. In the A zones, the WGCEP model predicts an earthquake rate about three times higher than that observed this century for **M**≥7 shocks, and five times higher than observed for **M**≥6.8 shocks (Fig. 10*a*). This, we believe, is the origin of the **M**≥7 earthquake deficit identified in the WGCEP report; it is a product of a model in which *b*=0.4 for **M**≤7.3 and *b*=2.2 for **M**>7.4. In contrast, the observed *b*-values of 0.9-1.2 are similar in all zones and all magnitude bands, with *b* values perhaps declining slightly off the San Andreas system (Fig. 10 and Table 3).

The moment rate predicted for each of the three zones by WGCEP (1995) is in good agreement with the observed moment rate during this century (Fig. 4*c*); no deficit is evident. This agreement, in concert with the absence of a significant difference between the moment release and accumulation rates (Fig. 9), removes any basis for WGCEP's conclusion that there is a deficit in the rate of large earthquakes that must be made up by aseismic creep, rare huge earthquakes, or a higher rate of **M**≥7 events.

Conclusions

WGCEP (1995) omitted several large earthquakes within its defined boundaries and used a minimum magnitude for which the catalog is incomplete, resulting in an underestimate of the rate of both **M**≥6 and **M**≥7 earthquakes. The more complete 1903-1996 **M**≥6 catalog presented here yields an earthquake rate 44% higher than the rate cited by WGCEP. We find that southern California has sustained 4-5 **M**≥6 shocks per decade and 4-5 **M**≥7 shocks per century. Although the earthquake rate varied sharply from one decade to the next during the 20th century, we find that this behavior is consistent with a Poisson process; there is no evidence that the rate of **M**≥6 earthquakes is increasing at the present time or at any other time during the 20th century.

The inferred rate of seismic moment release is dependent on the size and expected inter-event time of great earthquakes on the San Andreas fault, and the rate of moment accumulation rate is dependent on the depth extent over which seismic strain is stored. Though uncertain, we find that the rates of moment accumulation and release measured over both short and long time scales are not significantly different. There is no seismic moment deficit during the past 150 yr. We therefore find no evidence for a deficit in the rate of large earthquakes or seismic moment release.

In this paper we do not advocate a particular model for the distribution of earthquakes in space and time. Rather, it is our view that any model advanced must obey the observed frequency-magnitude relationship and earthquake production rate for the region (Fig. 3 and Table 3). This means that over 6.0≤**M**≤7.8, *b*=1.0 and *a*, the earthquake productivity rate, must lie between 5.5 and 6.0. This holds not only for the San Andreas fault but also for faults well off the major system (Fig. 10). We have thus sought to produce the most accurate and consistent catalog of earthquakes possible, and have used it to test a key model in use today.

Roughly half of the twentieth century **M**≥6 earthquakes have struck on the San Andreas system and half on the myriad secondary faults, with most of the seismic moment contributed by the largest earthquakes on the San Andreas system. In contrast, WGCEP (1995) concluded that the rate of **M**≥6 shocks on the lesser faults should be three times higher than what we have experienced during the past century. We suggest that the WGCEP distribution model suffered from insupportably high *b*-values for the minor faults. We thus find no evidence that huge (M~8), rare earthquakes strike southern California off the major faults. Nor do we see any need to invoke aseismic moment release to reconcile the observed rate of earthquakes with the driving motions of plate tectonics.

Acknowledgments: We thank James Savage, Susan Hough, Lucile Jones, Wayne Thatcher, Tousson Toppozada, Edward Field, Thomas Henyey, David Jackson, and Lind Gee for thoughtful reviews of this manuscript; Kerry Sieh for discussion on the San Andreas paleoseismic record; and Chuck Wicks for GMT expertise.

References

Agnew, D. C. (1991). How complete is the pre-instrumental record of earthquakes in southern California? In P. L. Abbott & W. J. Elliot (Eds.), *Environmental Perils of the San Diego Region* (pp. 75-88). San Diego: San Diego Assoc. Geologists (for Geol. Soc. Amer. Ann. Mtng).

Aki, K. (1965). Maximum likelihood estimate of *b* in the formula log N=*a*-*b*M and its confidence limits, *Bull. Earthquake Res. Inst.*, **43**, 237-239.

Allen, C. R., and J. M. Nordquist (1972). Foreshock, mainshock, and larger aftershocks of the Borrego Mountain earthquake. In *The Borrego Mountain Earthquake of April 9, 1968* (pp. 16-23). Washington: U.S. Geol. Surv. Prof. Paper 787.

Allen, C. R., P. St. Amand, C. F. Richter, and J. M. Nordquist (1965). Relationship between seismicity and geologic structure in the southern California region, *Bull. Seismol. Soc. Amer.*, **55**, 753-797.

Argus, D. F., and R. G. Gordon (1991). Current Sierra Nevada-North America motion from very long baseline interferometry: Implications for the kinematics of the western United States, *Geology*, **19**, 1085-1088.

Bakun, W. H., and T. V. McEvilly (1984). Recurrence models and the Parkfield, California, earthquakes, *J. Geophys. Res.*, **89**, 3051-3058.

Bath, M., and C. F. Richter (1958). Mechanisms of the aftershocks of the Kern County, California, earthquake of 1952, *Bull. Seismol. Soc. Amer.*, **48**, 133-146.

Beanland, S., and M. M. Clark (1994). The Owens Valley fault zone, eastern California, and surface faulting associated with the 1872 earthquake, *U.S. Geol. Surv. Bull. 1982.*.

Bennett, R. A., W. Rodi, and R. E. Reilinger (1996). Global Positioning System constraints on fault slip rates in southern California and northern Baja, Mexico, *J. Geophys. Res.*, **101**, 21,943-21,960.

Bent, A. L., and D. V. Helmberger (1991). A re-examination of historic earthquakes in the San Jacinto fault zone, *Bull. Seismol. Soc. Amer.*, **81**, 2289-2309.

Bent, A. L., and D. V. Helmberger (1989). Source complexity of the October 1, 1987, Whittier Narrows earthquake, *J. Geophys. Res.*, **94**, 9548-9556.

Bolt, B. A., A. Lomax, and R. A. Uhrhammer (1989). Analysis of regional broadband recordings of the 1987 Whittier Narrows, California, earthquake, *J. Geophys. Res.*, **94**, 9557-9568.

Burdick, L. J., and G. R. Mellman (1976). Inversion of the body waves from the Borrego Mountain earthquake to the source mechanism, *Bull. Seismol. Soc. Amer.*, **66**, 1485-1499.

Cao, T., M. D. Peterson, and M. S. Reichle (1996). Seismic hazard estimate from background seismicity in southern California, *Bull. Seismol. Soc. Amer.*, **86**, 1372-1381.

Chavez, D., J. Gonzales, A. Reyes, M. Medina, C. Duarte, J. N. Brune, F. L. Vernon III, R. Simons, L. K. Hutton, P. T. German, and C. E. Johnson (1982). Main-shock location and magnitude determination using combined U.S. and Mexican data. In *The Imperial Valley, California, earthquake of October 15, 1979* (pp. 51-54). Washington: U.S. Geol. Surv. Prof. Paper 1254.

Dehlinger, P., and B. A. Bolt (1987). Earthquakes and associated tectonics in a part of central California, *Bull. Seismol. Soc. Amer.*, **77**, 2056-2073.

DeMets, C. (1995). A reappraisal of seafloor spreading lineations in the Gulf of California: Implications for the transfer of Baja California to the Pacific plate and estimates of Pacific-North America plate motion, *Geophys. Res. Lett.*, **22**, 3545-3548.

Deng, J., and L. R. Sykes (1997). Evolution of the stress field in southern California and triggering of moderate-size earthquakes: A 200-year perspective, *J. Geophys. Res.*, **102**, 9859-9886.

Dollar, R. S., and D. V. Helmberger (1985). Body wave modeling using a master event for the sparsely recorded 1946 Walker Pass, California earthquake (abstract), *Eos, Am. Geophys. Union Trans.*, **66**, 964.

Donley, M. W., S. Allan, P. Caro, and C. P. Pattopn (1979). *Atlas of California*. Culver City: Pacific Book Center.

Doser, D. I. (1990a). A re-examination of the 1947 Manix, California, earthquake sequence and comparison to other sequences of the Mojave block, *Bull. Seismol. Soc. Amer.*, **80**, 267-277.

Doser, D. I. (1990b). Source characteristics of earthquakes along the southern San Jacinto and Imperial fault zones (1937 to 1954), *Bull. Seismol. Soc. Amer.*, **80**, 1099-1117.

Doser, D. I. (1992). Historic earthquakes (1918 to 1923) and an assessment of source parameters along the San Jacinto fault system, *Bull. Seismol. Soc. Amer.*, **82**, 1786-1801.

Doser, D. I. (1994). Contrasts between source parameters of M>5.5 earthquakes in northern Baja California (and Southern California), *Geophys. J. Int.*, **116**, 605-617.

Doser, D. I., and H. Kanamori (1986). Spatial and temporal variations in seismicity of the Imperial Valley (1902-1984), *Bull. Seismol. Soc. Amer.*, **76**, 421-438.

Dreger, D. (1997). The large aftershocks of the Northridge earthquake and their relationship to mainshock slip and fault-zone complexity, *Bull. Seismol. Soc. Amer.*, **87**, 1259-1266.

Eaton, J. P. (1990). 8. The earthquake and its aftershocks from May 2 through September 30, 1983. In *The Coalinga, California, earthquake of May 2, 1983* (pp. 113-170). Washington: U.S. Geol. Surv. Prof. Paper 1487.

Ebel, J. E., L. J. Burdick, and G. S. Stewart (1978). The source mechanism of the August 7, 1996 El Golfo earthquake, *Bull. Seismol. Soc. Amer.*, **68**, 1281-1292.

Ekström, G., R. S. Stein, J. P. Eaton, and D. Eberhart-Phillips (1992). Seismicity and geometry of a 110-km long blind thrust fault, 1, The 1985 Kettleman Hills, California, earthquake, *J. Geophys. Res.*, **97**, 4843-4864.

Ellsworth, W. L. (1990). Earthquake History, 1769-1989. In R. E. Wallace (Eds.), *The San Andreas fault System, California* (pp. 152-187). Washington: U.S. Geol. Surv. Prof. Pap. 1515.

Evans, R. D. (1955). *The Atomic Nucleus*. New York: MacGraw-Hill, 785 p.

Gawthrop, W. (1978). The 1927 Lompoc, California, earthquake, *Bull. Seismol. Soc. Amer.*, **68**, 1705-1716.

Gawthrop, W. (1981). Comments on "The Lompoc, California, earthquake (November 4, 1927; M = 7.3) and its aftershocks" by Thomas C. Hanks, *Bull. Seismol. Soc. Amer.*, **71**, 557-560.

Grant, L. B., and K. E. Sieh (1993). Stratigraphic evidence for seven meters of dextral slip on the San Andreas fault during the 1857 earthquake in the Carrizo Plain, *Bull. Seismol. Soc. Amer.*, **83**, 619-635.

Grant, L. B., and K. E. Sieh (1994). Paleoseismic evidence of clustered earthquakes on the San Andreas fault in the Carrizo Plain, California, *J. Geophys. Res.*, **99**, 6819-6841.

Gross, S., and S. Jaume (1995). *Historical seismicity of the southern Great Basin* (Rep. to Yucca Mtn. Proj., No. DTN GS950283117411.001). U.S. Dept. Energy.

Hanks, T. C. (1979). The Lompoc, California, earthquake (November 4, 1927; M = 7.3) and its aftershocks, *Bull. Seismol. Soc. Amer.*, **69**, 451-462.

Hanks, T. C. (1981). Reply to W. Gawthrop's "Comments on 'The Lompoc, California, earthquake (November 4, 1927; M = 7.3) and its aftershocks' ", *Bull. Seismol. Soc. Amer.*, **71**, 561-565.

Hanks, T. C. (1992). Small earthquakes, tectonic forces, *Science*, **256**, 1430-1432.

Hanks, T. C., and C. R. Allen (1989). The Elmore Ranch and Superstition Hills earthquakes of 24 November 1987: Intoduction to the special issue, *Bull. Seismol. Soc. Amer.*, **79**, 231-237.

Hanks, T. C., J. A. Hileman, and W. Thatcher (1975). Seismic moments of the larger earthquakes of the southern California region, *Geol. Soc. Amer. Bull.*, **86**, 1131-1139.

Hanks, T. C., and H. Kanamori (1979). A moment magnitude scale, *J. Geophys. Res.*, **84**, 2348-2350.

Hanks, T. C., and M. Wyss (1972). The use of body-wave spectra in the determination of seismic source parameters, *Bull. Seismol. Soc. Amer.*, **62**, 561-590.

Harris, R. A., and R. W. Simpson (1996). In the shadow of 1857-Effect of the great Ft. Tejon earthquake on subsequent earthquakes in southern California, *Geophys. Res. Letts.*, **23**, 229-232.

Hart, J. D. (1978). *A Companion to California*. New York: Oxford Univ. Press.

Hartzell, S. (1989). Comparison of seismic waveform inversion results for the rupture history of a finite fault: Application to the 1986 North Palm Springs, California, earthquake, *J. Geophys. Res.*, **94**, 7515-7534.

Hauksson, E., and S. Gross (1991). Source parameters of the 1933 Long Beach earthquake, *Bull. Seismol. Soc. Amer.*, **81**, 81-98.

Hauksson, E., and L. M. Jones (1989). The 1987 Whittier Narrows earthquake sequence in Los Angeles, southern California seismological and tectonic analysis, *J. Geophys. Res.*, **94**, 9569-9589.

Hauksson, E., L. M. Jones, and K. Hutton (1995). The 1994 Northridge earthquake sequence in California: Seismological and tectonic aspects, *J. Geophys. Res.*, **100**, 12,335-12,355.

Hauksson, E., L. M. Jones, K. Hutton, and D. Eberhart-Phillips (1993). The 1992 Landers earthquake sequence: Seismological observations, *J. Geophys. Res.*, **98**, 19835-19858.

Helmberger, D. V., P. G. Somerville, and E. Garnero (1992). The location and source parameters of the Lompoc, California, earthquake of 4 November 1927, *Bull. Seismol. Soc. Amer.*, **82**, 1678-1709.

Hileman, J. A., C. R. Allen, and J. M. Nordquist (1973). *Seismicity of the southern California region, 1 January 1932 to 31 December 1972* No. Seismol. Lab. Contrib. 2385). Calif. Institute of Technology, Pasadena (pp. Pages).

Hill, D. P., J. P. Eaton, and L. M. Jones (1990). Seismicity, 1980-1986. In R. E. Wallace (Eds.), *The San Andreas Fault System, California* (pp. 115-151). U.S. Geol. Surv. Prof. Pap.1515.

Hutton, L. K., and L. M. Jones (1993). Local magnitudes and apparent variations in seismicity rates in southern California, *Bull. Seismol. Soc. Amer.*, **83**, 313-329.

Jackson, D. D. (1996). The case for huge earthquakes (Opinion), *Seismol. Res. Lett.*, **67**, 3-5.

Jackson, D. D., Z.-K. Shen, D. Potter, X.-B. Ge, and L.-Y. Sung (1997). Southern California deformation, *Science*, **277**, 1621-1622.

Jones, L. E., S. E. Hough, and D. V. Helmberger (1993). Rupture process of the June 28, 1992 Big Bear earthquake, *Geophys. Res. Letts.*, **20**, 1907-1910.

Jones, L. M., and E. Hauksson (1997). The seismic cycle in southern California: Precursor or response?, *Geophys. Res. Lett.*, **24**, 469-472.

Jones, L. M., K. Hutton, D. A. Given, and C. R. Allen (1986). The July 1986 North Palm Springs, California, earthquake, *Bull. Seismol. Soc. Amer.*, **76**, 1830-1837.

Kanamori, H., and J. Regan (1982). Long-period surface waves. In *The Imperial Valley, California, earthquake of October 15, 1979* (pp. 55-58). Washington: U.S. Geol. Surv. Prof. Paper 1254.

King, G. C. P., R. S. Stein, and J. B. Rundle (1988). The growth of geological structures by repeated earthquakes, 1, Conceptual framework, *J. Geophys. Res.*, **93**, 13,307-13,318.

King, N. E., and W. Thatcher (1997). The coseismic slip distributions of the 1940 and 1979 Imperial Valley, California, earthquakes and their implications, *J. Geophys. Res.*, in press.

Kostrov, B. V. (1974). Seismic moment and energy of earthquakes, *Izv. Acad. Sci. USSR Phys. Solid Earth*, **1**, 23-40.

Magistrale, H., L. Jones, and H. Kanamori (1989). The Superstition Hills, California, earthquakes of 24 November 1987, *Bull. Seismol. Soc. Amer.*, **79**, 239-251.

Mueller, K. J., and T. K. Rockwell (1995). Late Quaternary activity of the Laguna Salada fault in northern Baja California, Mexico, *Geol. Soc. Amer. Bull.*, **107**, 8-18.

Nakanishi, I., and H. Kanamori (1984). Source mechanisms of twenty-six large, shallow earthquakes (Ms_6.5) during 1980 from P-wave first motion and long-period Rayleigh wave data, *Bull. Seismol. Soc. Amer.*, **74**, 805-818.

Nicholson, C. (1996). Seismic behavior of the southern San Andreas fault zone in the northern Coachella Valley, California: Comparison of the 1948 and 1986 earthquake sequences, *Bull. Seismol. Soc. Amer.*, **86**, 1331-1349.

Pacheco, J., and J. Nábelek (1988). Source Mechanisms of three moderate California earthquakes of July 1986, *Bull. Seismol. Soc. Amer.*, **78**, 1907-1929.

Pacheco, J. F., C. H. Scholz, and L. R. Sykes (1992). Changes in frequency-size relationship from small to large earthquakes, *Nature*, **355**, 71-73.

Petersen, M. D., W. A. Bryant, C. H. Cramer, T. Cao, and M. S. Reichle, A. D. Frankel, J. J. Lienkaemper, P. A. McCrory, and D. P. Schwartz (1996). Probabilistic seismic hazard assesement for the State of California, Calif. Div. Mines and Geol. Open-File Rep. 96-08 *and* U.S. Geol. Surv. Open-File Rep. 96-706.

Press, F., and C. Allen (1995). Patterns of seismic release in the Southern California region, *J. Geophys. Res.*, **100**, 6421-6430.

Richter, C. F. (1958). *Elementary Seismology*. San Francisco: W.H. Freeman & Co.

Salyards, S. L., K. E. Sieh, and J. L. Kirschvink (1992). Paleomagnetic measurement of nonbrittle coseismic deformation across the San Andreas fault at Pallett Creek, *J. Geophys. Res.*, **97**, 12,457-12,470.

Sanders, C. O., H. Magistrale, and H. Kanamori (1986). Rupture patterns and preshocks of large earthquakes in the southern San Jacinto fault zone, *Bull. Seismol. Soc. Amer.*, **76**, 1187-1206.

Satake, K., and P. G. Somerville (1992). Location and size of the 1927 Lompoc, California, earthquake from tsunami data, *Bull. Seismol. Soc. Amer.*, **82**, 1710-1725.

Savage, J. C., and M. Lisowski (1997). Viscoelastic coupling model of the San Andreas fault along the Big Bend, southern California, *J. Geophys. Res.*, in press.

SCEC (1996). Southern California Earthquake Center, J. Andrews (Ed.), *Is the rate of earthquakes increasing in California?* Los Angeles: Univ. So. Calif.

Sieh, K. (1996). The repetition of large earthquakes, *Proceed. U.S. Nat. Acad. Sci.*, **93**, 3764-3771.

Sieh, K. E. (1978). Slip along the San Andreas fault associated with the great 1957 earthquake, *Bull. Seismol. Soc. Amer.*, **68**, 1421-1448.

Sieh, K. E., and R. H. Jahns (1984). Holocene activity of the San Andreas fault at Wallace Creek, California, *Geol. Soc. Amer. Bull.*, **96**, 883-896.

Sipkin, S. A., and R. E. Needham (1990). Kinematic source parameters determined by time-dependent moment-tensor inversion and analysis of teleseismic first motions. In *The Coalinga, California, earthquake of May 2, 1983* (pp. 207-213). Washington: U.S. Geol. Surv. Prof. Paper 1487.

Stein, R. S., G. C. P. King, and J. B. Rundle (1988). The growth of geological structures by repeated earthquakes, 2, Field examples of continental dip-slip faults, *J. Geophys. Res.*, **93**, 13,319-13,331.

Stein, R. S., and W. Thatcher (1981). Seismic and aseismic deformation associated with the 1952 Kern County, California, earthquake and the relationship to the Quaternary history of the White Wolf fault, *J. Geophys. Res.*, **86**, 4913-4928.

Stirling, M. W., and S. G. Wesnousky (1997). Do historical rates of seismicity in southern California require the occurrence of earthquake magnitudes greater than would be predicted from fault length?, *Bull. Seismol. Soc. Amer.*, **87**, 1662-1667.

Strand, C. L. (1980) *Pre-1900 earthquakes of Baja California and San Diego County*. M.S. Thesis, 320 p., San Diego State Univ.

Sykes, L. R. (1996). Intermediate- and long-term earthquake prediction, *Proc. Natl. Acad. Sci USA*, **93**, 3732-3739.

Thatcher, W., and T. C. Hanks (1973). Source parameters of southern California earthquakes, *J. Geophys. Res.*, **78**, 8547-8576.

Toppozada, T. R. (1975). Earthquake magnitude as a function of intensity data in California and western Nevada, *Bull. Seismol. Soc. Amer.*, **65**, 1223-1238.

Toppozada, T. R. (1988). Earthquake history of California. In W. H. K. Lee, H. Meyers, & K. Shimazaki (Eds.), *Historical seismograms and earthquakes of the world* (pp. 267-265). San Diego, Calif.: Academic press.

Toppozada, T. R. (1995). History of damaging earthquakes in the Los Angeles and surrounding area, in M.C. Woods and W.R. Seiple, eds., The Northridge, California, Earthquake of 17 January 1994, Calif. Div. Mines and Geol. Spec. Pub. 116, 9-16.

Toppozada, T. R., and D. L. Parke (1982). Areas damaged by California earthquakes, 1900-1949, Calif. Div. Mines and Geol., Open-File Rep. 82-17, 65 p.

Toppozada, T. R., C. R. Real, and D. L. Parke (1981). Preparation of isoseismal maps and summaries of reported effects for pre-1900 California earthquakes, Calif. Div. Mines and Geol., Open-File Rep., 81-11 SAC, 182 p.

Tsai, Y.-B., and K. Aki (1969). Simultaneous determination of the seismic movement and attenuation of seismic surface waves, *Bull. Seismol. Soc. Amer.*, **59**, 275-287.

Velasco, A. M., C. J. Ammon, and T. Lay (1994). Empirical Green function deconvolution of broadband surface waves: Rupture directivity of the 1992 Landers, California (Mw=7.3) earthquake, *Bull. Seismol. Soc. Amer.*, **84**, 735-750.

Wald, D. J., and T. H. Heaton (1994). Spatial and temporal distribution of slip for the 1992 Landers, California earthquake, *Bull. Seismol. Soc. Amer.*, **84**, 668-691.

Wald, D. J., T. H. Heaton, and K. W. Hudnut (1996). The slip history of the 1994 Northridge, California, earthquake determined from strong-motion, teleseismic, GPS, and leveling data, *Bull. Seismol. Soc. Amer.*, **86**, S49-S70.

Ward, S. N. (1997). On the consistency of earthquake moment rates, geological fault data, and space geodetic strain: The United States, *Geophys. J. Int.*, submitted.

Wells, D. L., and K. J. Coppersmith (1994). New empirical relationships among magnitude, rupture length, rupture width, rupture area, and surface displacement, *Bull. Seismol. Soc. Amer.*, **84**, 974-1002.

WGCEP (1988). Working Group on California Earthquake Probabilities, Probabilities of large earthquakes occurring in California on the San Andreas fault, U.S. Geol. Surv. Open-File Rep. 88-398, 62 p.

WGCEP (1995). Working Group on California Earthquake Probabilities, Seismic hazards in southern California: Probable earthquakes, 1994-2014, *Bull. Seismol. Soc. Amer.*, **85**, 379-439.

Whitcomb, J. H., C. R. Allen, J. D. Garmany, and J. A. Hileman (1973). San Fernando earthquake series, 1971: Focal mechanisms and tectonics, *Rev. Geophys. Space Phys.*, **11**, 693-730.

Yeh, H.-C. (1975) *Mechanism of the 1927 Lompoc earthquake from surface wave analysis*. M.S., Univ. Washington, Seattle.

Appendix

This appendix provides a brief discussion and references for the locations, seismic moments, and focal mechanisms of the earthquakes given in Tables 1 and 2 and Fig. 1. Unless otherwise specified, locations and seismic moments are those given by Hanks et al (1975), with conversion from Mo to **M** following Hanks and Kanamori (1979). Times are shown when more than one earthquake occurs in one year.

1857 Fort Tejon. We use revised surface slip measurements (Grant and Sieh, 1993; Salyards et al., 1992; Sieh, 1978; Sieh and Jahns, 1984), and a rupture width (the down-dip dimension) equal to the local depth of contemporary microseismicity along the fault from Hill et al (1990). Microearthquakes extend to 12 km depth south of Parkfield, 15-20 km in the Carrizo Plain, 18-25 km at Tejon Pass, 12-15 km along the Mojave segment, and 17 km at Cajon Pass. For a shear modulus of 3.0 x 1010 Nm-2, this yields a moment of 7.7 x 1020 Nm (**M**=7.9). Deng and Sykes (1997) used 9.0 x 1020 Nm (**M**=7.9); Ellsworth (1990) assigned the earthquake **M**=7.8 (5.6 x 1020 Nm), which was adopted by WGCEP (1995).

1872 Owens Valley. Our location, focal mechanism, Mo and **M** estimates use the surface slip observations (Beanland and Clark, 1994), a fault width of 12.5 km, a dip of 80°E, and a shear modulus of 3.0x1010 Nm-2.

1892 Laguna Salada. Strand (1980) seems to have been the first to recognize the location of this event in the Laguna Salada, ~30 km south of the International Border at the longitude of El Centro. Earlier references customarily place this event on the Aqua Blanca fault, ~100 km to the south. Location and focal mechanism from Mueller and Rockwell (1995). Strand gives Mo=200 x 1018 Nm from AVI. Mueller and Rockwell give a minimum Mo of 42 x 1018 Nm, based on surface offsets. We use 100 x 1018 Nm.

1906 Imperial Valley. Considerable uncertainty still attends the location (Toppozada and Parke, 1982) and magnitude of this event. **M** is assigned from the Ms = 6.2 of Ellsworth (1990).

1907 San Bernardino. **M** < 6 assignment (Hanks et al., 1975; Toppozada and Parke, 1982).

1908 Death Valley. Location and magnitude very uncertain. **M** = 6? from Ellsworth (1990).

1910 Elsinore. **M**<6 assignment (Hanks et al., 1975; Toppozada and Parke, 1982).

1915 Imperial Valley (150623). Two earthquakes occurred on June 23, the first at 0359 and the second at 0456. Richter (1958) assigned **M** = 6 1/4 to each of them, but both Hanks et al (1975) and Toppozada and Parke (1982) find both of them to be **M** < 6 on the basis of AVI. Here we assign **M** = 6 to the first event and **M** < 6 to the second event, as did Ellsworth (1990). Put another way, we consider the strain release of both events to be the equivalent of one **M** = 6 event.

1915 Colorado River Delta (151121). Location, focal mechanism and moment from Doser (1994).

1916 Gorman (161023). **M** < 6 assignment (Hanks et al., 1975; Toppozada and Parke, 1982).

1916 Death Valley Region (161110). Richter (1958) did not list this event as **M** ≥ 6, although Ellsworth (1990) did. Gross and Jaumé (1995) find **M** = 5.9, principally because their new location is ~100 km closer to the seismic stations at Reno, Mount Hamilton, and Berkeley.

1918 San Jacinto. Hanks et al (1975) estimated Mo = 15 x 1018 Nm. Doser (1992) found Mo = 14 ± 5 x

1018 Nm from teleseismic body waves. Focal mechanism (Doser, 1992).

1922 Parkfield. Bakun and McEvilly (1984) find that the 1922, 1934, and 1966 Parkfield earthquakes are nearly identical. We assign them the same location, and same focal mechanism and Mo (Tsai and Aki, 1969).

1923 San Bernardino Area. Hanks et al (1975) estimate Mo = 1 x 1018 Nm. Doser (1992) finds Mo = 2 to 3 x 1018 Nm from a single teleseismic recording. In Table 1, we give Mo = 2 x 1018 Nm and **M**=6.2. Focal mechanism (Doser, 1992).

1927 Lompoc, offshore. Both the location and size of this earthquake have been sources of considerable controversy. The location of this event is that of Hanks (1979), but interested readers may wish to examine Gawthrop (1978), Gawthrop (1981), Hanks (1981). Mo estimates for this earthquake vary by an order of magnitude. In units of 1018 Nm and in chronological order, these estimates are 100 (Hanks et al., 1975), 65 (Yeh, 1975), 10 (Helmberger et al., 1992), and 30 (Satake and Somerville, 1992). Our "consensus" Mo is 50 x 1018 Nm and **M** = 7.1. Focal mechanism (Yeh, 1975).

1933 Long Beach. Location, focal mechanism, and Mo (Hauksson and Gross, 1991).

1934 Parkfield (340608). Location (Bakun and McEvilly, 1984). Focal mechanism and Mo (Tsai and Aki, 1969). See 1922 Parkfield above.

1934 Colorado River Delta (341230). Location, focal mechanism and moment from Doser (1994).

1934 Colorado River Delta (341231). Location, focal mechanism and moment from Doser (1994).

1937 Anza, southeast. Location (Sanders et al., 1986). **M**_6 assignment Hanks et al (1975); Doser (1990b).

1940 Imperial Valley. Location (Doser and Kanamori, 1986). Hanks et al (1975) give Mo = 30 x 1018 Nm; Doser (1990b) give 23 ± 4 x 1018 Nm, and King and Thatcher (1997) find 32±3 x 1018 Nm from geodetic inversion; we use 30 x 1018 Nm. Focal mechanism (Doser, 1990b).

1942 Lower Borrego Valley (421021). Location (Hanks and Allen, 1989) based on the earlier determinations (Doser and Kanamori, 1986; Hanks et al., 1975; Sanders et al., 1986), exactly that given by Richter (1958). We use Mo = 5 x 1018 Nm, based on the estimates of 9 x 1018 Nm (Hanks et al., 1975), 1.5 ± 0.5 x 1018 Nm (Doser, 1990b) and 3.3 x 1018 Nm (Bent and Helmberger, 1991). Focal mechanism (Doser, 1990b).

1942 Salton Sea aftershock (421022). This event is nominally an aftershock of the significantly larger lower Borrego Valley earthquake, which occurred 7.5 hours earlier, but it occurred far to the northeast, beneath the Salton Sea. Perhaps it possesses a relationship to the Lower Borrego Valley earthquake that is similar to that between the 1987 Elmore Ranch and Superstition Hills earthquake (Hanks and Allen, 1989). This event is a marginal entry in Table 1, with *M*L=5.5 (Hileman et al., 1973), but Bent et al (1991) have determined Mo = 1.5 x 1018 Nm. We list 1 x 1018 Nm, **M** = 6, here. Location (Doser and Kanamori, 1986; Hileman et al., 1973).

1946 Walker Pass. Location (Richter, 1958). Mo (Hanks et al, 1975). The focal mechanism is for a more recent event to which the 1946 earthquake seems to conform (Dollar and Helmberger, 1985). The master event location is 35°45'N, 118°03'W.

1947 Manix. Location, focal mechanism, and Mo (Doser, 1990a).

1948 Desert Hot Springs. Location, focal mechanism, and Mo (Nicholson, 1996).

1952 Kern County, mainshock (520721) Location, Mo and focal mechanism (Stein and Thatcher, 1981).

1952 Kern County, aftershock (520721). This event (Table 2) occurred on July 23, 1952. According to Thatcher and Hanks (1973), Mo = 0.4 x 1018 Nm for this event and **M**<6.

1952 Kern County, aftershock (520729). Location and focal mechanism (Bath and Richter, 1958).

1952 Bryson (521122). Location and focal mechanism (Dehlinger and Bolt, 1987). Magnitude (Ellsworth, 1990).

1954 Arroyo Salada. Location (Richter, 1958; Sanders et al., 1986). Focal mechanism (Doser, 1990b). Mo = 3 x 1018 Nm (Hanks et al., 1975), 2.4 ± 0.3 x 1018 Nm (Doser, 1990b), 1.9 x 1018 Nm (Bent and Helmberger, 1991).

1966 Parkfield (660628). Location (Bakun and McEvilly, 1984). Focal mechanism and Mo (Tsai and Aki, 1969).

1966 El Golfo, Baja California, Mexico (660807). Location, Mo, focal mechanism (Ebel et al., 1978).

1968 Borrego Mountain. Location and focal mechanism (Allen and Nordquist, 1972). Mo (Burdick and Mellman, 1976; Hanks and Wyss, 1972).

1971 San Fernando. Location and focal mechanism (Whitcomb et al., 1973).

1979 Imperial Valley. Location and focal mechanism (Chavez et al., 1982). Mo (Kanamori and Regan, 1982).

1980 Victoria, Baja California (Mexico). Location, Mo, and focal mechanism (Nakanishi and Kanamori, 1984).

1983 Coalinga. Location and focal mechanism (Eaton, 1990). Mo *(Sipkin and Needham, 1990)*.

*1985 Kettleman Hills. Location, focal mechanism, and M*o (Ekström et al., 1992).

1986 North Palm Springs. Location (Jones et al., 1986). Focal mechanism and Mo *(Pacheco and Nábelek, 1988). Hartzell (1989) finds M*o *to be 1.6 to 1.8 x 10*18 Nm. We prefer **M**=6, given that ML = 5.9 (Jones et al., 1986).

1987 Whittier Narrows (871001). Location (Hauksson and Jones, 1989). Focal mechanism (Bent and Helmberger, 1989). Mo (Bent and Helmberger, 1989; Bolt et al., 1989).

1987 Elmore Ranch (871124). Location (Magistrale et al., 1989). Focal mechanism and Mo (Sipkin, 1989;

Bent et al, 1989).

1987 Superstition Hills (871124). Location (Magistrale et al, 1989) Focal mechanism and Mo (Sipkin, 1989; Bent et al, 1989).

1992 Joshua Tree (920423). Location ([Hauksson et al, 1993). Focal mechanism and Mo (Velasco et al., 1994).

1992 Landers (920628). Location (Hauksson et al., 1993). Focal mechanism and Mo (Velasco et al., 1994; Wald and Heaton, 1994).

1992 Big Bear (920628). Location (Hauksson et al., 1993). Focal mechanism and Mo (Jones et al., 1993).

1994 Northridge (940117). Location (Hauksson et al., 1995). Focal mechanism and Mo (Wald et al., 1996).

1994 Northridge aftershock (940117). Location, focal mechanism and Mo (Dreger, 1997).

Table 1. 1903-1997 **M**_6.0 Southern California Catalog (32°00'-36°15'N/114°00'-122°00'W)

Locality	Yr	Mo	Dy	Latitude		Longitude		*WGCEP*	Focal mechanism			Mo	**M**
				deg	min	deg	min	zone	strike °	dip °	rake °	1018Nm	
Imperial Valley	06	4	19	32	54	115	30	B	-	-	-	2	6.2
Death Valley	08	11	4	36	?	117	?	C	-	-	-	1?	6 ?
Imperial Valley	15	6	23	32	48	115	30	B	-	-	-	1	6.0
Volcano Lake (Baja)	15	11	21	32	0	115	0	C	312	88	179	9	6.6
San Jacinto	18	4	21	33	45	117	0	A	150	87	-176	15	6.8
Parkfield	22	3	10	36	0	120	30	B	327	90	180	1	6.0
San Bernardino	23	7	23	34	0	117	15	A	320	85	180	2	6.2
Santa Barbara	25	6	29	34	18	119	48	C	-	-	-	20	6.8
Lompoc	27	11	4	34	36	120	54	C	315	42	94	50	7.1

Long Beach	33	3	11	33	42	118	0	B	315	80	-170	5	6.4
Parkfield	34	6	8	36	0	120	30	B	327	90	180	1	6.0
Laguna Salada (Baja)	34	12	30	32	15	115	30	B	311	91	80	6	6.5
Colorado River delta	34	12	31	32	0	114	45	B	317	89	180	40	7.0
Imperial Valley	40	5	19	32	48	115	30	B	325	90	180	30	7.0
Lower Borrego Valley	42	10	21	33	0	116	0	A	61	88	10	5	6.4
Salton Sea aftershock	42	10	22	33	12	115	42	B	-	-	-	1	6.0
Walker Pass	46	3	15	35	42	118	6	C	346	45	-117	1	6.0
Manix	47	4	10	35	0	116	36	C	65	85	8	6	6.5
Desert Hot Springs	48	12	4	33	54	116	24	A	305	70	169	1	6.0
Kern County	52	7	21	35	0	119	0	B	73	75	50	110	7.3
Kern Co. aftershock	52	7	21	35	0	119	0	B	-	-	-	3	6.3
Kern Co. aftershock	52	7	29	35	24	118	54	C	53	90	-	3	6.3
Bryson	52	11	22	35	42	121	12	C	305	63	175	1	6.0
Arroyo Salada	54	3	19	33	18	116	12	A	307	85	175	3	6.3
Parkfield	66	6	28	36	0	120	30	B	327	90	180	1	6.0
Borrego Mountain	68	4	9	33	11	116	8	A	312	83	180	10	6.6
San Fernando	71	2	9	34	25	118	24	B	293	52	72	10	6.6
Imperial Valley	79	10	15	32	38	115	19	B	326	90	180	6	6.5
Victoria (Baja)	80	6	9	32	13	114	59	B	140	90	180	5	6.4
Coalinga	83	5	2	36	14	120	19	C	127	23	90	5	6.4
Kettleman	85	8	4	36	7	120	9	C	142	12	109	2	6.2

Hills													
North Palm Springs	86	7	8	34	0	116	37	A	283	41	147	1	6.0
Whittier Narrows	87	10	1	34	4	118	5	A	280	40	98	1	6.0
Elmore Ranch	87	11	24	33	5	115	48	A	217	79	4	2	6.2
Superstition Hills	87	11	24	33	1	115	51	A	303	89	-180	10	6.6
Joshua Tree	92	4	23	33	58	116	18	C	171	89	-177	2	6.2
Landers	92	6	28	34	12	116	26	C	341	70	-172	110	7.3
Big Bear	92	6	28	34	10	116	49	C	321	86	200	5	6.5
Northridge	94	1	17	34	13	118	32	B	122	40	101	13	6.7
Northridge aftershock	94	1	17	34	20	118	41	B	116	46	89	1	6.0

References can be found in the Appendix. Earthquakes are mapped in Figs. 1 and 2; WGCEP seismotectonic zones are shown in Fig. 2. Unknown focal mechanisms are blank.

Table 2. What's Not in Table 1

Year	Mo	Dy	Locality	Lat.(°)	Lon.(°)	*M_6*	Ref.	**M<6**	Ref.
1907	09	20	San Bernardino	34.2?	117.1?	6	R	5.3	HHT
								5.3	TP
1910	05	15	Elsinore	33.7?	117.4	6	R	5.3	HHT
								5 1/2	TP
1915	06	23	Imperial Valley (0456)	32.8	115.5	6 1/4	R	5.5	HHT
								5.9	TP
1916	10	23	Gorman	34.9	118.9	6	R	5.3	HHT
								5.3	TP
1916	11	10	Death Valley area	35.3?	116.7	6.1	E	<6	R
								5.9	GJ
1935	02	24	Laguna Salada (Baja)	32.0	115.2	6	R	<6	HHT
1937	03	25	Southeast Anza	33.5	116.4	6	R	5.6	HHT
								5.6	D

1952	07	23	Kern Co. aftershock	35.4	118.6	6.1	R	5.7	TH
Year	Mo	Dy	Locality	Lat.(°)	Lon.(°)	Mo (10^{20} Nm)		**M**	Ref.
1857	01	09	Fort Tejon	35.7	120.3	8		7.9	S, GS
1872	03	26	Owens Valley	36.7	118.1	2		7.4	BC
1892	02	24	Laguna Salada	32.5	116.6	1		7.3	S, MR

The first section lists **M**<6 earthquakes and the second lists **M**_7 shocks occuring during 1850-1900 within Fig. 1. References: R (Richter, 1958), HHT (Hanks et al., 1975), TP (Toppozada and Parke, 1982), E (Ellsworth, 1990), GJ (Gross and Jaume, 1995), TH (Thatcher and Hanks, 1973), D (Doser, 1990), S (Sieh, 1978), GS (Grant and Sieh, 1994), BC (Beanland and Clark, 1994), S (Strand, 1980), MR (Mueller and Rockwell, 1995). Also see Appendix.

Table 3. Frequency-Magnitude Relationships for the **M**≥6.0 Southern California Catalog

Seismotectonic		Min. Magnitude	by Maximum Likelihood		by Least Squares	
Zone	*n*	of completeness	*b*	*a*	*b*	*a*
All	40	6.0	0.97±0.15	5.45	1.04±0.04	5.89
All	42	6.0 ?	1.01±0.16	5.73	1.04±0.04	5.93
All	28	6.2	1.04±0.20	5.91	1.11±0.04	6.38
A	10	6.0	1.21±0.38	6.26	1.25±0.14	6.56
B	17	6.0	0.95±0.23	4.97	0.97±0.07	5.10
C	13	6.0	0.86±0.24	4.31	0.87±0.04	4.41

n is the number of earthquakes in each set. *a* is in units of yr^{-1}. ? Assumes the 1903-1997 catalog is missing two **M**=6.0 earthquakes.